

# Voltage and Current Inversion Challenges When Protecting Series-Compensated Lines – A Case Study

Eric Bakie and Curtis Westhoff, *Idaho Power*  
Normann Fischer and Jordan Bell, *Schweitzer Engineering Laboratories, Inc.*

**Abstract**—In order to increase power transfer capabilities, Idaho Power is upgrading two existing 230 kV series-compensated transmission lines from 28 percent compensation to 70 percent compensation.

Protecting series-compensated lines is both a science and an art. This paper discusses the voltage and current inversion aspect of series-compensated lines where very little literature is available. A voltage inversion will challenge the security and dependability of both the directional and distance protection elements, whereas a current inversion will challenge the directional, distance, and differential protection elements. This paper will endeavor to add to the literature regarding how to adequately protect series-compensated lines where the possibility of current inversion exists.

Using series compensation to increase power transfer capabilities of transmission paths requires advanced simulation tools to ensure the reliability of line protection systems. This paper describes how to leverage transient simulation tools and a Real Time Digital Simulator to develop and verify optimized protection settings for series-compensated transmission lines prone to current inversion.

## I. INTRODUCTION

With the goal of increasing the total transfer capability of an internal transmission path, Idaho Power recently increased the series compensation level on two existing 230 kV transmission lines located in southern Idaho. The prior series capacitor bank equipment was at the end of its useful life (installed in 1966 and approaching 50 years old) and scheduled for replacement as part of an aging infrastructure replacement program. Instead of replacing the existing equipment with similar-sized series capacitor banks, the project provided an opportunity to upgrade the transfer capability of an internally operated Idaho Power transmission path by increasing both the ampacity rating and compensating impedance of the new series capacitor banks. Installed compensation on the two lines increased from 28 to 70 percent of the transmission line impedance. This translates into an increase of approximately 17 to 42 ohms of capacitive reactance. The upgrade increased the nominal ampacity rating of the banks from 1,283 to 1,600 amperes (511 megawatts to 637 megawatts) and increased the emergency ampacity rating of the banks from 1,730 to 2,160 amperes (690 megawatts to 860 megawatts).

The capacitor banks are of a gapless design protected by metal oxide varistors (MOVs) installed in parallel with the capacitors. The series capacitor bank protection includes high-current bypass logic for internal faults and high-energy bypass logic for external faults. The MOVs limit the voltage across the

capacitors during short-circuit and transient events on the transmission system. A bypass breaker, installed in parallel with the MOVs, bypasses the bank as a protective action when the current through the MOV exceeds the high-current threshold or when the energy dissipated by the MOV exceeds the energy threshold.

The MOVs have sufficient capacity to absorb the worst case energy and conduct the worst case fault current during internal and external faults. For internal faults, the breaker bypasses the bank at high speed, which reduces the total amount of energy the MOVs need to dissipate. The high-speed bypassing of the capacitor bank for internal faults is also beneficial to the line protection. The system does not require a full bypass for the worst case external faults, which improves system stability. MOV energy requirement studies are typically performed considering different power flow scenarios and the impact of point-on-wave on fault initiation. In addition to the MOV energy requirements identified in the studies, installing extra MOV capacity provides energy margins should MOV columns fail or the system fault duty increase.

For the new installation, Idaho Power discovered that the short-circuit voltage across the capacitor bank was below the knee point of the MOV characteristic for close-in internal line-to-line faults. Therefore, the MOV high-current logic pickup setting in the capacitor bank protection system was greater than the expected MOV current levels for close-in internal line-to-line faults. Initial analysis identified that current inversion was the primary cause of the reduced fault current levels during close-in line-to-line faults. Under a current inversion scenario, the distance protection elements cannot detect the fault, because the calculated impedance appears in the reverse direction to the line relay. A severe current inversion can also negatively impact line current differential schemes, which are primarily compensated at one end and require additional analysis to properly set the line current differential operate and restraint quantities.

Reduction of the compensation level in order to reduce the current inversion severity was not an acceptable option. Idaho Power needed the additional compensation level in order to achieve the desired transmission capacity improvements.

Idaho Power pursued a solution for overcoming the protection challenges presented to line relaying elements during current inversion using a two-part approach: 1) evaluate power system and capacitor bank MOV protection system

performance using transient simulations in PSCAD™, 2) evaluate line relaying performance of the line current differential element using the results of the PSCAD model and simulations in a closed-loop testing environment using a Real Time Digital Simulator (RTDS®).

The engineering analysis resulted in optimized settings for the line current differential protection elements capable of protecting the series-compensated lines during a current inversion at the desired 42 ohm (70 percent) compensation level.

## II. THEORY OVERVIEW

The simplified power transfer equation (1) governs the power transfer between two transmission line terminals. This equation neglects the influence of the transmission line resistance.

$$P = \frac{V_1 V_2 \sin(\theta_{12})}{X_L} \quad (1)$$

where:

- P = Power transferred between line terminals
- V<sub>1</sub> = Voltage magnitude at Terminal 1
- V<sub>2</sub> = Voltage magnitude at Terminal 2
- θ<sub>12</sub> = Angular difference between V<sub>1</sub> and V<sub>2</sub>
- X<sub>L</sub> = Inductive reactance of the transmission line

If we assume V<sub>1</sub> and V<sub>2</sub> are fixed (the system voltage remains within 95 to 105 percent of the nominal value) and θ<sub>12</sub> is defined by the power system, the only parameter power system designers can alter with regard to power transfer is the transmission line impedance. To increase the power transmission capability between two substations in a power system, one of the following must occur: either an additional transmission line needs to be built or the impedance of the existing transmission line or lines needs to decrease. Constructing an additional transmission line or lines is cost prohibitive and involves a considerable delay because of permitting requirements. Therefore, the most viable option is to reduce the impedance of the existing transmission lines. Transmission line impedance is predominantly inductive. To negate this inductance, we insert a capacitor in series with the transmission line to decrease the overall transmission line impedance. The impact of adding the series capacitor can be shown by modifying (1) to incorporate the capacitive reactance of the series capacitor as shown in (2).

$$P = \frac{V_1 V_2 \sin(\theta_{12})}{X_L - X_C} \quad (2)$$

where:

- X<sub>C</sub> = Capacitive reactance of the series capacitor

Series compensation increases the power transfer capability of a transmission line, which results in an increased power system stability margin. However, series compensation introduces a new set of challenges for power system and protection engineers. The series combination of the capacitor and inductance of the transmission line creates a resonant circuit with a resonant frequency (f<sub>RES</sub>) given by (3).

$$f_{RES} = \frac{1}{2\pi\sqrt{LC}} = f_{NOM} \sqrt{\frac{X_C}{X_L}} \quad (3)$$

where:

- f<sub>NOM</sub> = Nominal frequency of the power system

Typically the X<sub>C</sub>/X<sub>L</sub> ratio is in the range of 0.25 to 0.8; therefore, the resonant frequency will be a subharmonic of the power system frequency [1] [2]. Any disturbance in the power system, be it a switching condition or fault, will excite the power system at this subharmonic frequency. The disturbance will in turn give rise to transient currents at this frequency. These subharmonic transient currents interact with the synchronous generators of the power system and develop an oscillating or pulsating torque in the rotor. The frequency of this oscillating torque is equal to the difference between the nominal frequency of the power system (f<sub>NOM</sub>) and the resonant frequency (f<sub>RES</sub>) of the inductor capacitor circuit (LC). If the difference between these two frequencies coincides with one of the torsional modes of the generator's shaft system, torsional oscillations will be excited. This phenomenon is known as subsynchronous resonance (SSR). Multistage steam turbines are most susceptible to SSR, because these typically have four to five torsional frequencies. If no preventive measures are taken, SSR can lead to generator shaft failure [3].

Series capacitors are exposed to a large range of fault currents. A large fault current results in a large voltage drop across the capacitor, which can result in damage to the series capacitor if not addressed. To prevent damage to the series capacitor during large transient fault currents, series capacitors are equipped with spark gaps or an MOV in parallel with the series capacitor. The MOV clamps the magnitude of the voltage across the series capacitor to within the operational limits of the series capacitor. Fig. 1 shows a sketch of a series capacitor overvoltage protection circuit [4].

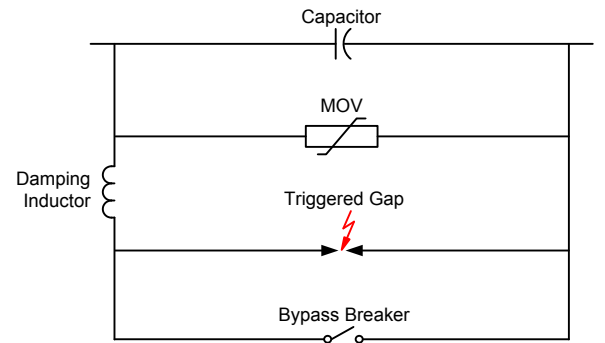


Fig. 1. Sketch of an MOV-protected series capacitor including the damping inductor and the controlled spark gap (gap shown for illustration).

During normal system operating conditions, when the voltage drop across the capacitor is lower than the MOV reference voltage, the MOV behaves for all practical purposes as an open circuit. However, if the voltage drop across the capacitor begins to increase and exceeds the MOV reference voltage, the MOV begins to conduct and behaves like a variable resistor with the resistance value being inversely proportional

to the voltage drop across the series capacitor. When the MOV resistance changes, the effective capacitance of the series capacitor begins to decrease. In his 1987 paper [4], Goldsworthy shows that the parallel combination of a capacitor and MOV are equivalent to the series combination of a resistor ( $R_C$ ) and the capacitive reactance ( $X_{C_C}$ ). Fig. 2 shows an equivalent circuit, known as the Goldsworthy equivalent circuit.

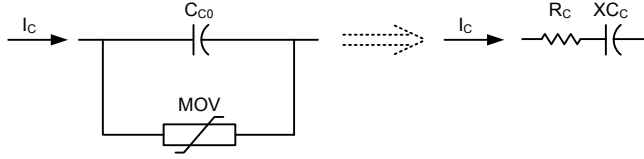


Fig. 2. Capacitor in parallel with MOV and the equivalent series impedance circuit at fundamental frequency.

The values of the  $R_C$  and  $X_{C_C}$  in the Goldsworthy equivalent circuit are dependent on the through-current of the capacitor ( $C_{C0}$ ). Fig. 3 shows a plot of  $R_C$  and  $X_{C_C}$  versus current. The impedance of the capacitor at fundamental frequency serves as the impedance base, and the rated current of the series capacitor serves as the current base.

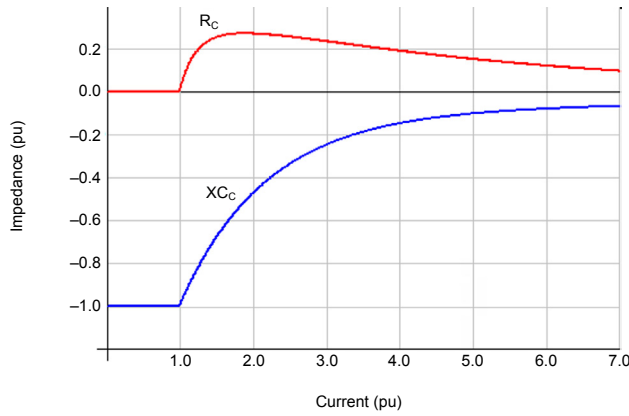


Fig. 3. Plot of the variation of  $R_C$  and  $X_{C_C}$  versus current in the Goldsworthy equivalent circuit.

From Fig. 3, we can see how  $R_C$  and  $X_{C_C}$  vary with respect to current. The variation of  $R_C$  and  $X_{C_C}$  is of particular concern from the point of view of distance protection and fault location, because the fault current can vary as a result of changes in the source impedance or fault resistance. To demonstrate the effect of  $R_C$  and  $X_{C_C}$  variation on impedance-based elements (distance or fault locating), consider the simple power system in Fig. 4. The transmission line is series compensated in the middle of the line by 70 percent.

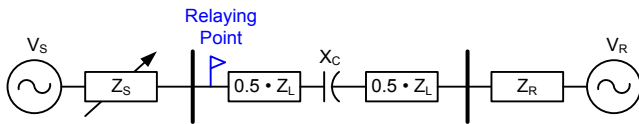


Fig. 4. Sketch of a simple power system with a midline series-compensated transmission line.

If we now plot the impedance as calculated by a distance element for a fault at the end of the line for varying values of fault current (fault current is varied by changing the source

impedance  $Z_S$ ), we obtain a sample set of plots as shown in Fig. 5. From Fig. 5, we can see that the impedance calculated by a distance element for a fault at the end of the line varies considerably. In each case, the distance element overreaches with the worst overreach occurring at low values of fault current.

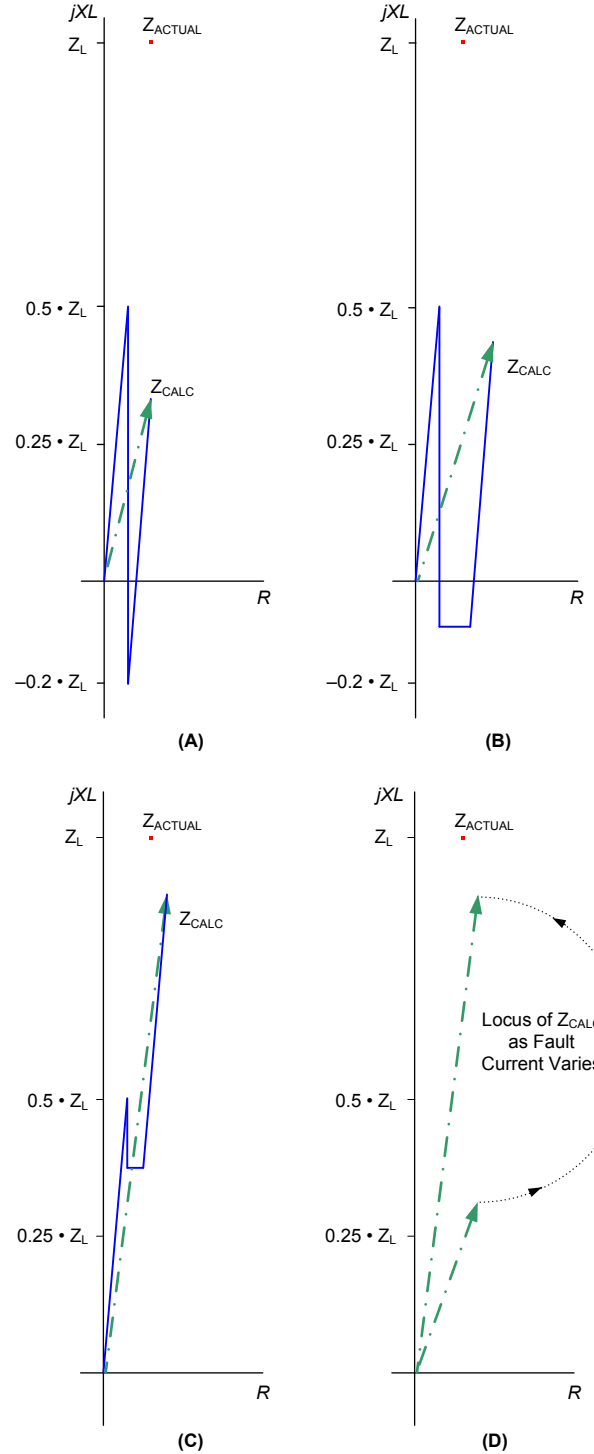


Fig. 5. Plots of the impedance calculated by the distance element for faults at the end of the line for varying values of fault current: (A) fault current is below the rated current of the series capacitor, (B) fault current is approximately 1.5–2.0 pu of rated current, (C) fault current is 6–7 pu of rated current, and (D) locus of impedance calculation for variation of fault current.

How can we provide protection for a series-compensated transmission line without overreaching? Before we answer this question, let's consider two further issues with regard to series-compensated transmission lines.

#### A. Voltage Inversion

For a fault on a series-compensated transmission line, if the impedance between the fault point and the relaying point is capacitive but the overall impedance between the power system source and fault point is still inductive, the power system will experience what is known as a voltage inversion. Depending on the location of the potential transformer (PT), the protective relay may measure this voltage inversion. To understand why this voltage inversion occurs, consider Fig. 4. Assume that the power system experiences a bolted fault 60 percent from the relaying point as shown in Fig. 6.

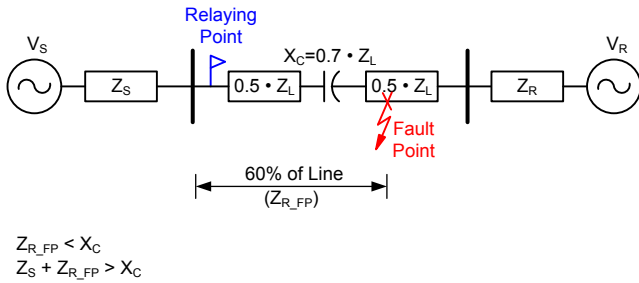


Fig. 6. Sketch of a simple power system with the transmission line being series compensated at the line terminal.

Because the impedance between the source ( $V_S$ ) and the fault point is inductive, the fault current supplied by the source will be inductive, i.e., the fault current will lag source voltage by the line angle (assuming a homogeneous power system). If we calculate the voltage drop across each of the power system components, knowing the voltage at the fault is zero (solid bolted fault), we obtain the voltage profile shown in Fig. 7.

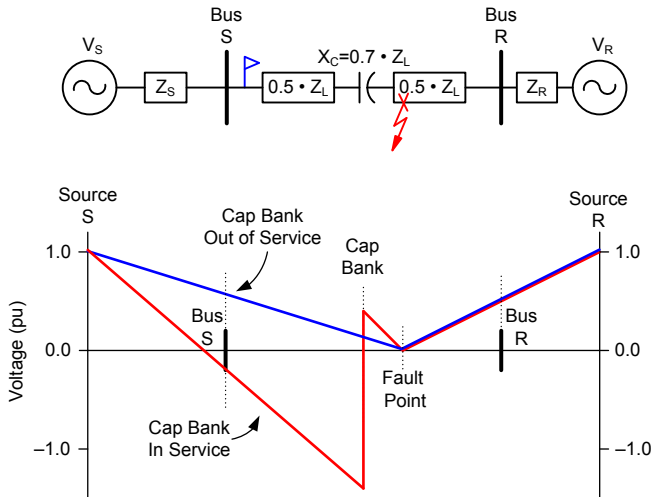


Fig. 7. The voltage profile across the simple power system of Fig. 6 with the series capacitor bank in service (red) and the series capacitor bank out of service (blue).

The plot also contains the voltage profile across the power system with the series capacitor out of service or bypassed. Note that a negative voltage does not denote a negative

magnitude but rather a voltage that is out-of-phase with the source voltage or a voltage inversion.

If we examine the voltage at the relaying point (Bus S in Fig. 7), we can make the following observations about the out-of-service and in-service capacitor banks. When the capacitor bank is out of service, the voltage at the relaying point for the fault is reduced in magnitude but still of the same sign (in phase) as the voltage at the source (Source S). However, when the capacitor bank is in service, the voltage at the relaying point is of the opposite sign (out of phase) with the source voltage, causing the voltage inversion. What is the effect or impact of the voltage inversion at the relaying point when the series capacitor bank is in service? To answer this question, let us examine the relationship between the voltage and current during a fault condition when the series capacitor bank is in service and when it is out of service. Fig. 8 shows a sketch of the relationship between the voltage and current for the two different cases. Note that all phasor drawings reflect a counterclockwise power system rotation.

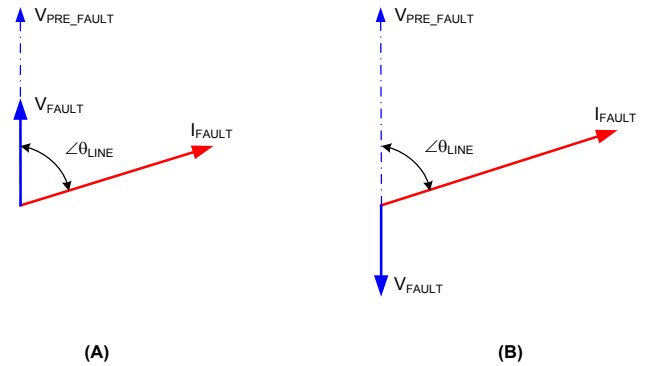


Fig. 8. Phasor relationship between the faulted phase voltage and current at Bus S when (A) the series capacitor bank is out of service and (B) the series capacitor bank is in service.

A power system is primarily inductive. A bolted fault in front of the relaying point will result in the current lagging the voltage by the transmission line angle ( $\angle\theta_{LINE}$ ) for a homogeneous power system. A bolted fault behind the relaying point will result in the current leading the voltage by  $180^\circ - \angle\theta_{LINE}$ . In Fig. 8(A), we see that the current lags the voltage by the transmission line angle. A voltage-polarized distance element would identify the fault as being in the forward direction, which is correct because the fault is in front of the relay. However, in Fig. 8(B), the current leads the voltage, and a voltage-polarized distance element could identify the fault in the reverse direction if the polarizing voltage followed the faulted phase voltage. Therefore, a voltage inversion on the power system can result in a distance element that is polarized by voltage to incorrectly declare the fault direction.

To overcome this issue, modern distance relays use memory voltage to polarize the distance element. The memory voltage time constant needs to be carefully selected so the memory voltage is not corrupted during the fault, resulting in loss of security and dependability of the distance element [5]. The memory voltage resolves the inverted voltage issue by polarizing the distance element with the prefault memorized

voltage but does not address the overreaching issue of the distance element.

An interesting observation about a voltage inversion is that it does not affect the negative- or zero-sequence directional elements, because the source impedance ( $Z_S$ ) remains inductive. Assume the simple power system in Fig. 6 experiences an A-phase-to-ground fault. Fig. 9(A) shows the phase relationship between the phase voltages before and during the fault and the phase relationship between the zero- and negative-sequence currents and voltages during the fault when the series capacitor bank is not in service. As expected for a fault in front of the relay measuring point, the negative- and zero-sequence currents lead the negative- and zero-sequence voltages by a phase angle greater than 90 degrees but less than 180 degrees. Fig. 9(B) shows the same phase relationships but this time with the series capacitor bank in service.

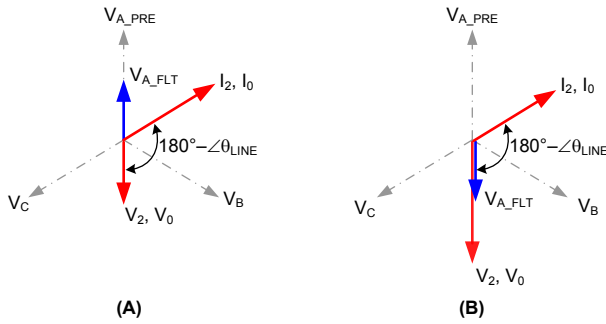


Fig. 9. Phasor relationship between the negative- and zero-sequence voltages and currents at Bus S when (A) the capacitor bank is out of service and (B) the capacitor bank is in service.

If we compare the phase relationship between the negative- and zero-sequence currents and voltages in Fig. 9(B), we see it is the same as that in Fig. 9(A). The phase relationship between the negative- and zero-sequence voltages and currents is not affected by a voltage inversion. The voltage inversion actually aids the sequence directional elements, because it boosts the negative- and zero-sequence voltage quantities.

### B. Current Inversion

In a power system with series compensation, the possibility exists that for a fault on the power system, the impedance between the power system source and fault point can be capacitive. If this occurs, the fault current will be capacitive instead of inductive. This phenomenon is known as a current inversion. A current inversion does not only impact the current during the fault condition, but it also impacts the voltage profile on the power system. For a better understanding of this phenomenon, let us again use a simple power system but with a transmission line that is series compensated at one of the line terminals. Fig. 10 shows a sketch of a simple power system in which current inversion can occur.

A sketch of the phase relationship between the fault current and voltage for a fault on the power system as shown in Fig. 10 is shown in Fig. 11. For comparison, the phase relationship between the voltage and current when the capacitor bank in Fig. 10 is out of service is also shown in Fig. 11.

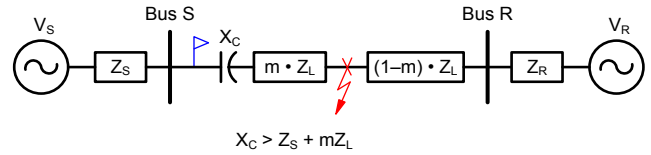


Fig. 10. Sketch of a simple power system in which current inversion can occur.

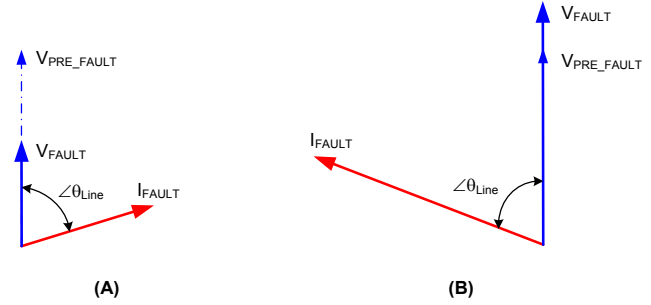


Fig. 11. Phasor relationship between the faulted phase voltage and current at Bus S when (A) the capacitor bank is out of service and (B) the capacitor bank is in service.

Examining Fig. 11(B), we notice that the current leads the voltage by the line angle (compared to lagging the voltage by the line angle), and the fault voltage magnitude during the fault increases compared to the magnitude of the prefault voltage. The first observation, that the current leads the voltage by the line angle, would be true for the current flowing into the line at Bus S (Fig. 10), because the impedance between the source and fault point is capacitive. However, this would not be the case for the current flowing into Bus R, because the impedance between the fault and its source is still inductive. Therefore, the current at Bus R will lag the voltage by the line angle. If we use the voltage at Bus S as a reference and plot the phasor relationship between the current flowing into the line at Bus S and R as shown in Fig. 12, we soon realize that this relationship has the same signature as an external fault.

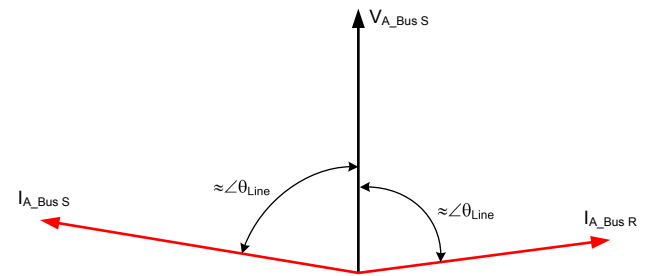


Fig. 12. The phasor relationship between the voltage at Bus S and the fault currents flowing into Bus S and Bus R for an internal line fault during a current inversion.

The second observation from Fig. 11(B) is that the fault voltage increases in magnitude with respect to the prefault voltage. Fig. 13 is a sketch of the voltage profile across the power system during the fault condition.



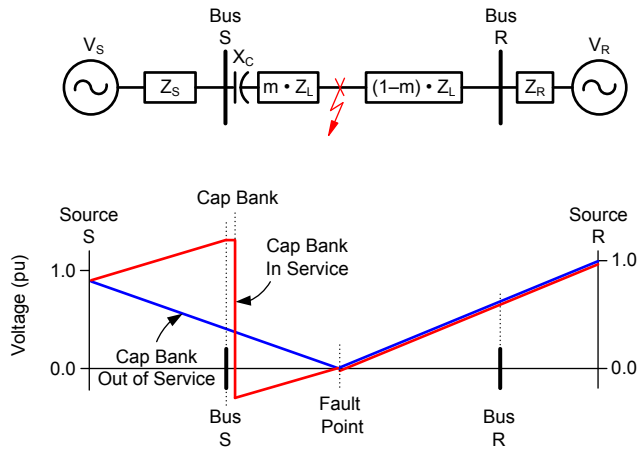


Fig. 13. The voltage profile across the simple power system of Fig. 10 with the series capacitor bank in service (red) and the series capacitor bank out of service (blue).

During a current inversion, the voltage magnitude on portions of the power system increases rather than decreases. When a capacitive current flows through an inductive impedance, the voltage drop across the inductive circuit is out of phase with the source voltage. If we subtract this voltage drop from the source voltage, we effectively add the voltage drop to that of the source, resulting in a voltage increase across a portion of the power system. However, power systems are not designed to operate at voltage magnitudes above 150 percent of the nominal voltage rating of the power system (such operation would result in failure of equipment insulation). In order to prevent power system equipment failure resulting from excessive voltage, power systems are fitted with surge arrestors to keep the voltage magnitude within safe operating levels. Therefore, the voltage profile shown in Fig. 13 is possible only in theory. In practice, however, the voltage on the power system will not exceed 150 percent of nominal.

Generally, the magnitude of the fault current that flows through the series capacitor during a current inversion is well above the operating current of the series capacitor bank (six to seven times the rated current). Therefore, the voltage drop across the series capacitor far exceeds the MOV reference voltage ( $V_{REF}$ ). This large voltage drop decreases the MOV resistance to a very small value (well below the impedance of the series capacitor), causing the MOV to effectively bypass the series capacitor. During the time period that the series capacitor is bypassed by the MOV, the impedance between the source and the fault point becomes once again inductive and greater in magnitude than when the series capacitor is in service. Therefore, the fault current becomes inductive and decreases in magnitude. This causes a voltage drop across the power system that is approximately in phase with the source voltage and results in a voltage lower than the source voltage across the power system. In general, a current inversion on a power system lasts less than one power system cycle. Fig. 13 also shows that when a current inversion occurs, the power system will also experience a voltage inversion.

At the beginning of this section we asked the question—if distance elements are prone to overreaching on series-compensated lines, how can we best make protection secure

while not overreaching? A line differential protection scheme would seem to be the preferred choice; however, power systems with series-compensated lines are prone not only to voltage inversions but also to current inversions. So, how can we best protect transmission lines that are series compensated? The following case study of the Idaho Power transmission system, which is compensated at one terminal, will answer this question.

### III. SYSTEM MODEL

To evaluate the performance of any proposed protection scheme, we must first subject the scheme to a full suite of different fault and operating conditions. To realize this, we must build a model of the power system under study to simulate operation of that system in an electromagnetic transient environment. The single-line diagram of the power system model used for the Idaho Power electromagnetic transient studies is shown in Fig. 14. The positive-sequence source impedances for the two substations, Substation A and Substation B, are approximately  $j7.9$  ohms and  $j12.3$  ohms, respectively. The positive-sequence line impedances for both transmission lines (ZL2 and ZL3) are approximately  $j60.8$  ohms each. The reactance of the two series capacitors (XC232 and XC233) is  $-j42$  ohms each.

Recall, this is an existing line where modern microprocessor relays with digital communications capabilities are installed at each of the line terminals. Each of the parallel series-compensated transmission lines has a dual primary protection scheme. The first main protection on both lines is a permissive overreaching transfer trip scheme that uses distance protection elements. A line current differential element provides a secondary main protection scheme. Using Fig. 14, the manufacturer of the series capacitor bank developed a network model in PSCAD to perform transient simulations for designing and evaluating the performance of the series capacitor bank MOV protection system.

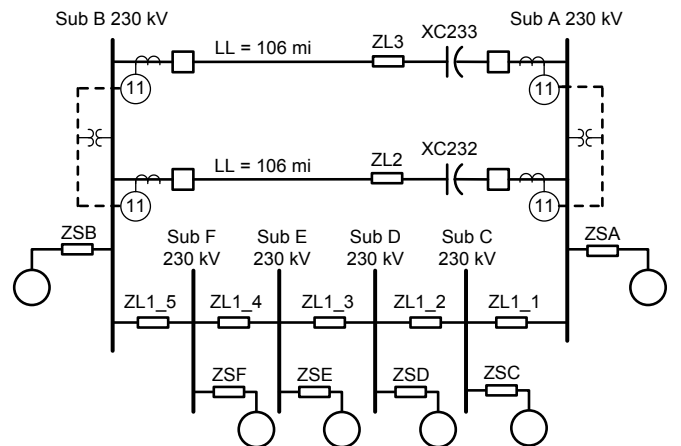


Fig. 14. Single-line diagram of the system model used for transient simulations.

#### IV. INITIAL RELAY ANALYSIS

While developing new settings for the line relays associated with the series capacitor replacement project, Idaho Power made several observations for close-in line-to-line faults:

- The series capacitor impedance was limiting the fault current magnitude.
- The series capacitor impedance was limiting the voltage drop across the capacitor bank line-to-line to levels below or near the knee point of the MOV characteristic. This was preventing the MOV from conducting sufficient current to bypass the series capacitor.
- The inability of the series capacitor bank protection system to detect close-in internal fault conditions and issue a bypass command exposes the line protection relay elements to current inversion. A current inversion condition causes the line relaying elements to incorrectly calculate the fault as being outside the zone of protection.

Idaho Power requested the transient simulation results for various scenarios in COMTRADE format from the series capacitor bank manufacturer to verify that the MOVs would conduct and that the capacitor bank would bypass for close-in internal faults. System performance was evaluated during close-in line-to-line faults using the PSCAD model and transient simulation for heavy and light power flow cases.

The minimum peak MOV current was determined for both the heavy and light power flow cases for sixty-one different point-on-wave fault scenarios. Three of the sixty-one line-to-line fault simulations resulted in a peak MOV current less than the bypass logic pickup setting during heavy loading conditions. For the light load power flow case, fifteen of the sixty-one simulations resulted in a peak MOV current less than the bypass pickup. Fig. 15 shows the transient simulation results for the MOV current for the worst case power flow scenario.

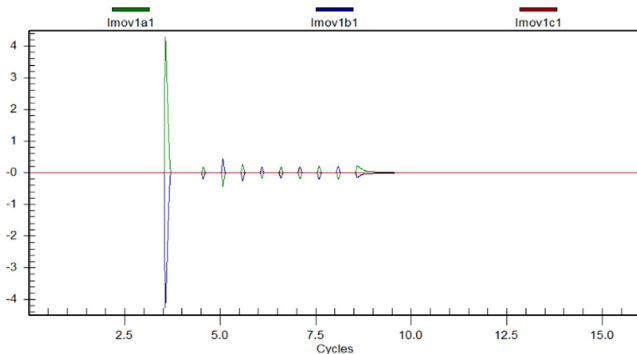


Fig. 15. Minimum peak MOV current for the worst case internal fault location, type, and fault initiation angle.

At the beginning of the fault, the MOV conducts for a very short duration and reaches a peak value of 4.3 kA, a level below the high-current bypass pickup value of 5.9 kA. Thus, for this scenario, the series capacitor bank is not bypassed.

The high-current bypass setting for the MOV is set at 115 percent of the worst case expected external fault current.

Lowering the bypass setting was not an option, because the MOV current for the close-in fault scenarios was less than 80 percent of the largest expected external fault current. Therefore, lowering the bypass setting would have resulted in triggering bypass circuitry of the series capacitor during an external fault condition. This is an undesirable operation that would interfere with the power transfer capability of the system. Another solution was necessary to resolve this issue.

Without the ability to bypass the series capacitor bank for close-in internal faults, the power system will experience a current inversion. The impedance between the source and fault point will be capacitive. This results in the fault current flowing in a direction away from the fault instead of toward the fault. Fig. 16 shows an example of a current inversion at Substation A during a simulated fault on the power system.

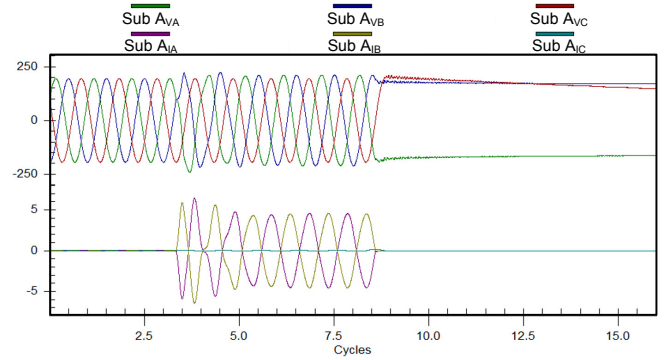


Fig. 16. Substation A voltage and current waveforms during current inversion conditions.

Notice that the current reverses phase shortly after fault initiation. Also note that the bus voltage magnitude is not depressed during the fault state. While this fault may be difficult for the protective relay to detect, it is not a very severe fault for the system.

The distance relays will calculate the fault to be in the reverse direction under this scenario. Normally, current inversion is not a concern for distance relays on series-compensated lines, because the capacitive current is usually very large in magnitude leading to a fast bypass of the series capacitor. For the Idaho Power system, however, the capacitance is large enough in relation to the small source impedance of the system that the fault is near or below the minimum bypass level of the capacitor bank protection system.

To illustrate the impact of current inversion on distance elements, a transient simulation of a close-in line-to-line fault that resulted in no capacitor bank bypass was played back into a short-circuit program relay model. Fig. 17 shows the response of the distance element. The measured apparent impedance does not enter the forward-looking operating characteristic; it begins and settles in the reverse direction. Forward-looking distance protection elements at the series-compensated terminal will not detect faults when there is a current inversion.

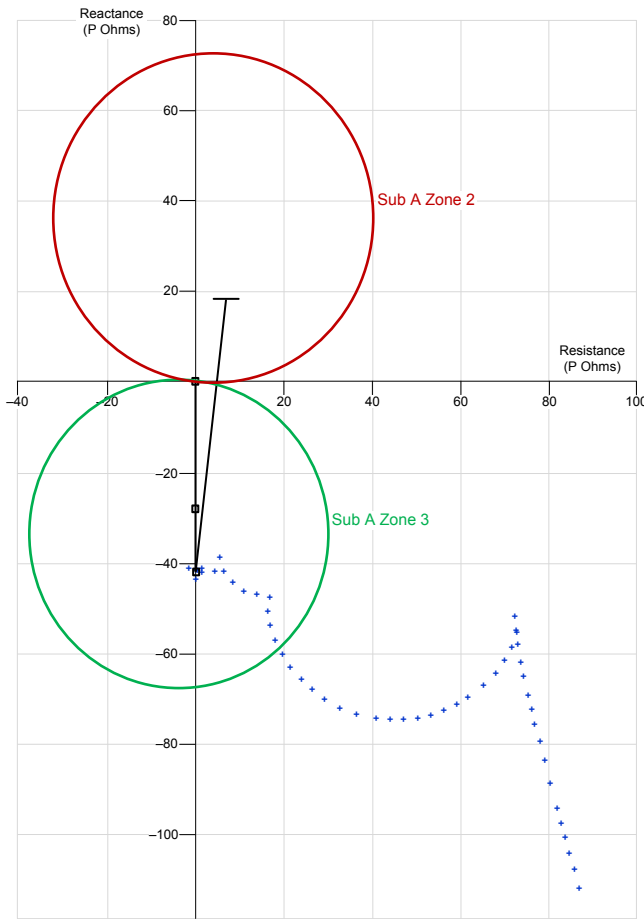


Fig. 17. Substation A distance element response for a line-to-line fault without a series capacitor bank bypass.

The line protection system also included line current differential elements that used an alpha plane characteristic. Fig. 18 shows the alpha plane characteristic.

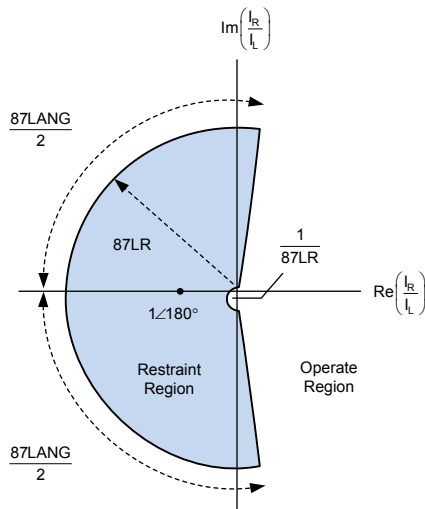


Fig. 18. Alpha plane relay characteristic for the line current differential relay element.

The area in blue is the restraint region,  $I_R$  is the remote terminal current,  $I_L$  is the local terminal current,  $87LANG$  is the blocking angle, and  $87LR$  is the blocking radius.

Initial steady-state short-circuit study results presented doubt that the line current differential scheme could be set to detect internal fault conditions, resulting in current inversion. The sending and remote terminal fault current angles were nearly 180 degrees apart, and furthermore, the sending-to-receiving fault current magnitude was a 1.7 to 1 ratio. Given the installed relays have a minimum alpha plane radius setting (87LR) of 2.0, it looked unlikely that the line current differential relays could be set with a reduced restraint region to detect the current inversion.

Idaho Power took a closer look at the network impedance values and the line current differential element to gain a better understanding. They then calculated the maximum restraining slope for a percent differential element [6]. The calculated values indicated that the maximum restraining slope for a percent differential characteristic for this system was 36.3 percent. The percent differential characteristic was then transferred to the alpha plane based on the transformation equations described in [7]. A 36.3 percent differential restraining slope corresponds to an 87LR setting of 2.136 on an alpha plane characteristic. Fig. 19 shows the 36.3 percent differential restraining slope using an alpha plane characteristic.

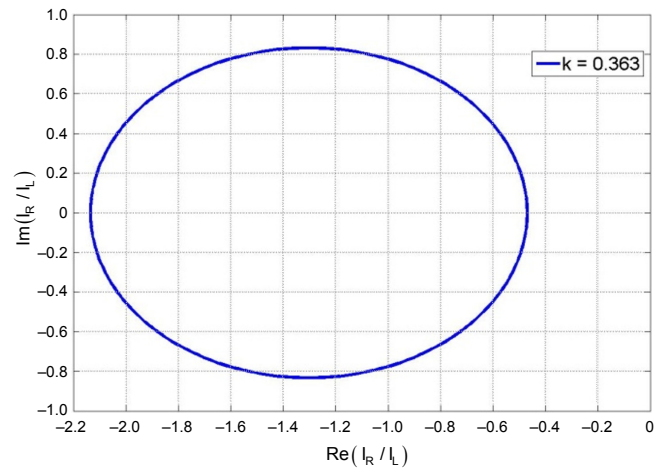


Fig. 19. Percent differential ( $k = 0.363$ ) referenced to an alpha plane relay characteristic.

Idaho Power noticed that following fault initiation, the fault was inductive on the initial transient before moving to the capacitive current steady state. This observation led Idaho Power to conduct a transient performance analysis of the line current differential relay to determine if a protection solution could be reached. Using the various transient simulation scenarios provided by the capacitor bank manufacturer as specified by Idaho Power, we tried answering two questions:

- 1) What was the magnitude of the differential current?
- 2) How long was the fault trajectory in the alpha plane operate region?

Idaho Power first calculated the differential current for two different transient simulation scenarios to determine if the differential current was in the operate region of the alpha plane. Next, they determined if the magnitude of the differential current was above the 87LPP supervisory setting. Finally, they



calculated the time duration while both conditions were satisfied for two different 87LR settings.

Idaho Power also performed current transformer (CT) saturation analysis of external fault conditions that could cause a false differential current. They found CT saturation was not a risk.

Table I shows a summary of the initial analysis of the transient simulations for case study one (scenario one). Fig. 20 shows a plot of the differential current for case study one. Fig. 21 shows the A-phase alpha plane operating characteristic and fault trajectory for case study one as measured at Substation A.

TABLE I  
INITIAL TRANSIENT SIMULATION ANALYSIS OF THE LINE CURRENT  
DIFFERENTIAL CHARACTERISTIC FOR CASE STUDY ONE

Analysis	Initial Settings	Adjusted Settings
AB fault, line-side of XC232	87LR = 6.0	87LR = 2.0
Time in operate region	0.216 cycles	1.005 cycles
Mag. Idiff > 87LPP while in operate region?	Yes	Yes
Time in operate region and above 87LPP pickup setting	0.216 cycles	1.005 cycles

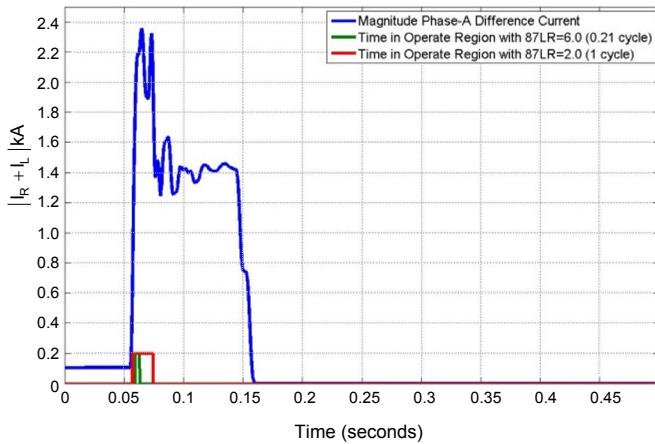


Fig. 20. Substation A difference current for initial transient analysis of a line-to-line fault for case study one.

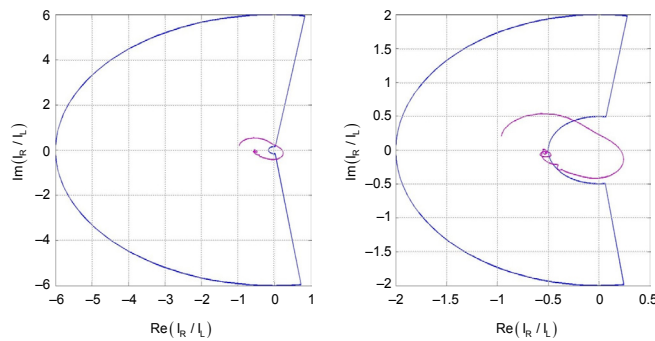


Fig. 21. Fault trajectory for a line-to-line fault at Substation A for various 87LR settings for case study one.

The initial transient analysis for case study one suggested that reducing the restraining radius setting provided a benefit for detecting the line-to-line fault during current inversion.

Table II shows a summary of the initial analysis of the transient simulations for case study two (scenario two), which was the worst case of all the scenarios considered. Note that the initial operating point is in the operate region due to minimum power transfer. For this operating point, the primary component of the line current is due to line charging. Fig. 22 shows a plot of the difference current for case study two. Fig. 23 shows the A-phase alpha plane operating characteristic and fault trajectory for case study two as measured at Substation A.

TABLE II  
INITIAL TRANSIENT SIMULATION ANALYSIS OF THE LINE CURRENT  
DIFFERENTIAL CHARACTERISTIC FOR CASE STUDY TWO

Analysis	Initial Settings	Adjusted Settings
AB fault, line-side of XC232	87LR = 6.0	87LR = 2.0
Time in operate region	3.78 cycles	3.80 cycles
Mag. Idiff > 87LPP while in operate region?	Yes	Yes
Time in operate region and above 87LPP pickup setting	0.303 cycles	0.303 cycles

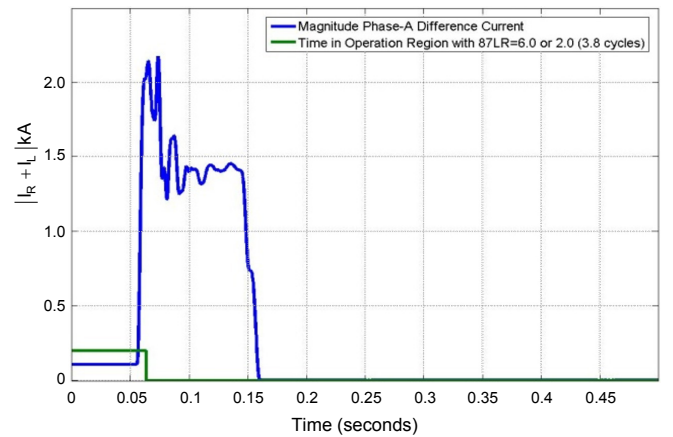


Fig. 22. Substation A difference current for initial transient analysis of a line-to-line fault for case study two.

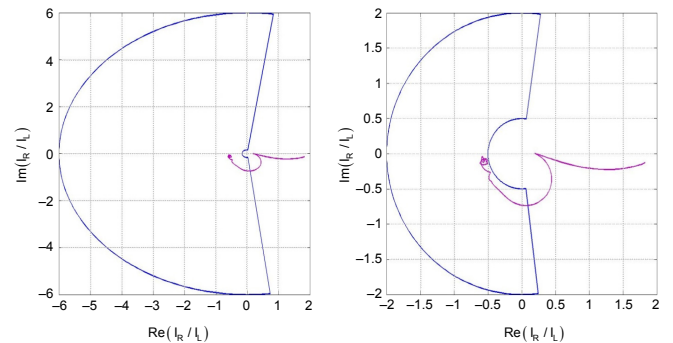


Fig. 23. Fault trajectory for a line-to-line fault at Substation A for various 87LR settings for case study two.

The initial transient analysis for case study two suggested that reducing the restraining radius setting did not provide a benefit for detecting the line-to-line fault during the current inversion; thus additional analysis was necessary.

The initial transient analysis for both case studies indicated the line current differential relay would pick up for a short duration. To be certain, however, a detailed analysis of the actual relay performance during transient conditions and current inversion conditions was necessary. Idaho Power contacted the relay manufacturer to perform RTDS testing to verify that the actual relay performance would allow for trip operation.

The initial testing consisted of COMTRADE files provided from a PSCAD model. The currents are in perspective from the primary side; Fig. 24 shows the magnitude and angle.

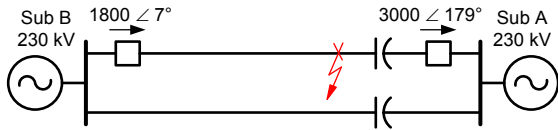


Fig. 24. Test system one-line diagram for verifying trip operation.

The relay manufacturer played these files into the relays and analyzed the relay event records. Fig. 25 shows an event record of the faulted phase currents. The first quarter-cycle shows that the local currents, IAL and IBL, and the remote currents, IAX and IBX, are about to come in phase with one another, indicating an internal fault. However, by one half-cycle, the fault currents shift to become almost 180 degrees out of phase, indicating the A- and B-phase differential elements (87LA and 87LB respectively) did not operate for the fault. The negative-sequence differential element operates with the same behavior; however, it was not analyzed in this scenario. The negative-sequence differential element is built for sensitivity, whereas the phase differential element is built for speed.

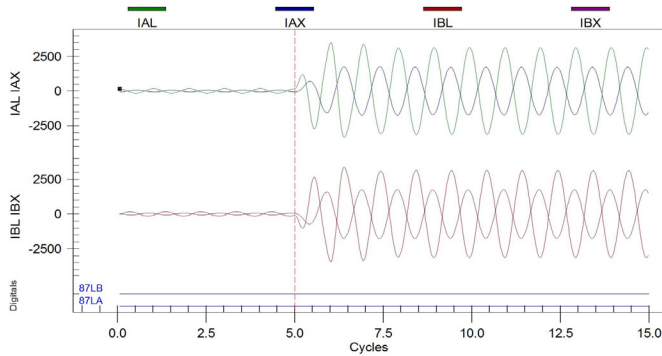


Fig. 25. Faulted phase currents for the line-to-line fault.

The magnitudes of the phase differential currents were then examined to view their behavior. The phase differential currents are shown in Fig. 26.

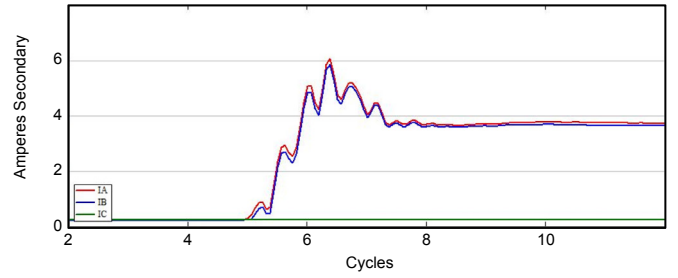


Fig. 26. Differential current magnitude for all phases.

The magnitudes of the A- and B-phase differential currents peak near the differential pickup of six amperes and settle out just below four amperes secondary in the steady state. The alpha plane was examined next to understand the impedance trajectory during the fault. This is shown in Fig. 27.

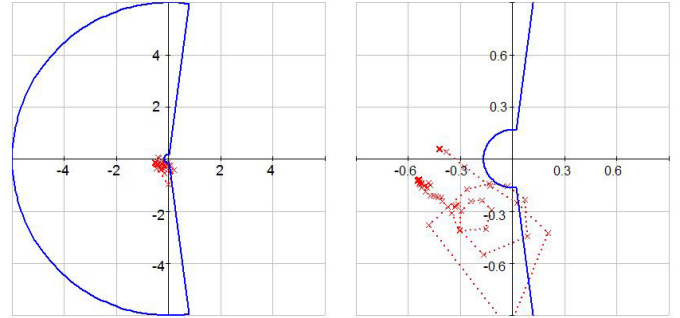


Fig. 27. A-phase alpha plane during the fault.

During the fault, the remote-to-local ratio briefly oscillates in the operate region for a couple sample points before coming to a steady state in the restraint region.

## V. SEARCH FOR A DEPENDABLE SOLUTION

Using the RTDS allowed for quick testing and verification of the various relay elements that would be set to find a viable solution.

### A. Differential Pickup

The differential current pickup had to be adjusted to a lower value so it would be below the differential current produced during the fault. Originally, the phase element pickup was set to the default of six amperes, or 1.2 per unit. The relay phase differential calculation during steady state after the transients subsided was just below four amperes, so a lower value had to be selected for the phase pickup. A value of 2 amperes (0.4 per unit) was selected and the fault was applied again. Fig. 28 shows the resulting event record.

With the decreased pickup value, the differential elements were able to assert for the fault for a duration of 0.188 cycles, approximately three milliseconds. While one processing interval is all that is required for the relay to operate, a longer assertion of the differential element is desirable.

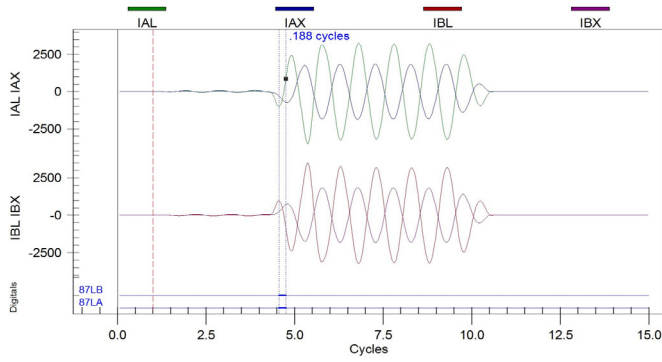


Fig. 28. Relay operation with reduced differential pickup.

### B. Blocking Angle

The blocking angle originally used was 195 degrees. While in the majority of cases this is a suitable setting to use, decreasing it would allow for more of the subharmonic oscillations to be in the operate region. This setting was decreased to 100 degrees; Fig. 29 shows the results on the alpha plane.

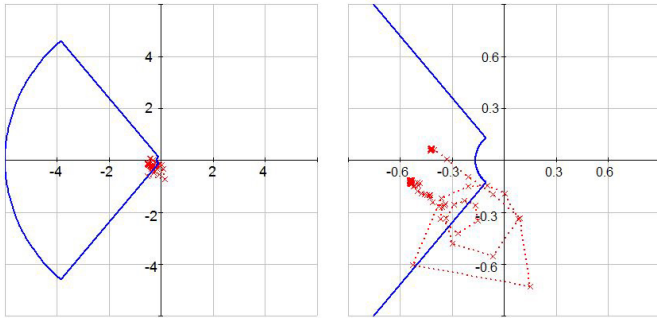


Fig. 29. Alpha plane with reduced blocking angle.

Decreasing the angle created more samples in the operate region and allowed for the differential element to be asserted for 0.625 cycles, approximately 10 milliseconds, with a momentary dropout. Fig. 30 shows the effect of this on the differential element.

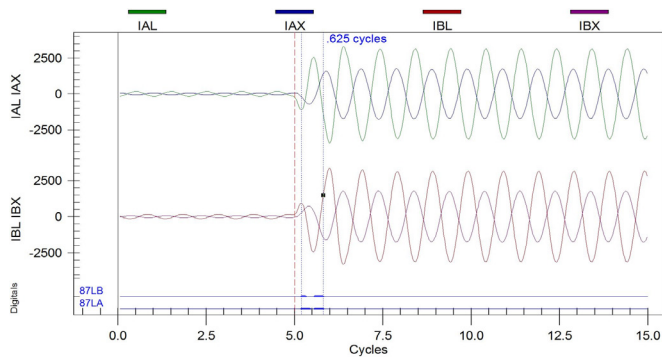


Fig. 30. Relay operation with reduced blocking angle.

### C. Blocking Radius

The blocking radius originally used for the outer radius was 6, giving an inner radius of 1/6. Fig. 31 shows the result of reducing the setting to give an outer radius of 2 and an inner radius of 1/2.

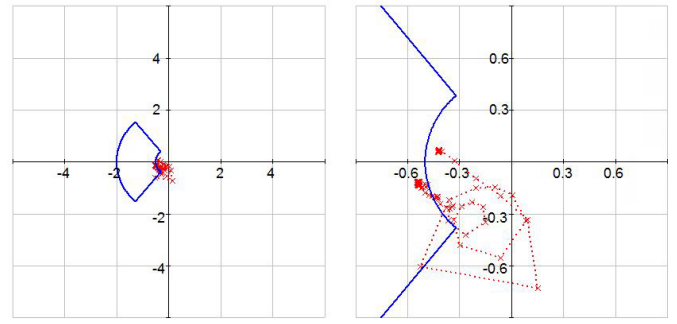


Fig. 31. Alpha plane with reduced blocking radius.

Decreasing the radius created more samples in the operate region. Fig. 32 shows the effect on the differential element.

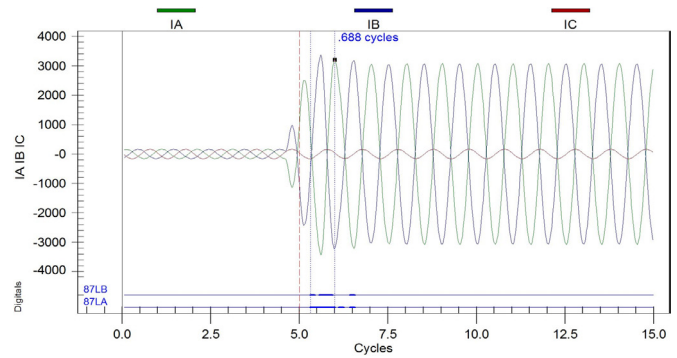


Fig. 32. Relay operation with reduced blocking radius.

The differential elements were asserted for a solid 0.688 cycles, approximately 11.5 milliseconds, and intermittently for a total of 1.25 cycles, providing a more dependable operation for the phase elements.

### D. Result

A dependable solution was found by adjusting all three components of the differential element: pickup, blocking angle, and blocking radius. The negative-sequence differential has an intentional security delay that prevents it from operating in this transient condition.

## VI. DIFFERENTIAL ELEMENT SECURITY

With the settings validated to operate for internal faults, it was necessary to prove security of the element with the applied settings for external faults. Single-line-to-ground, double-line-to-ground, line-to-line, and three-line-to-ground faults were applied on the bus local to the series capacitor and on the adjacent line on the line-side of the capacitor. Fig. 33 shows the fault locations.

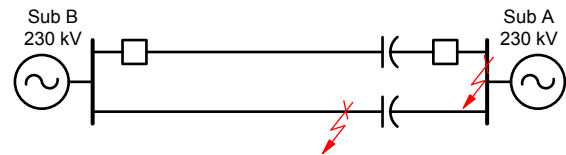


Fig. 33. External fault locations for the element security tests.

Fig. 34 to Fig. 37 show the results of the differential currents for the applied faults.

### A. Bus Faults at Substation A

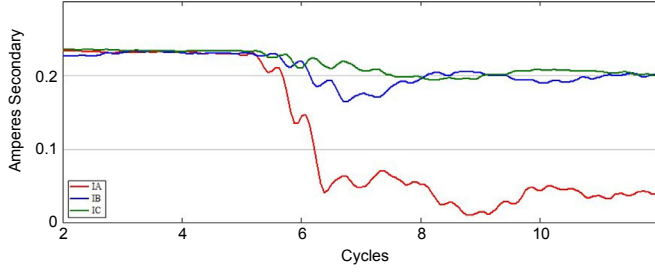


Fig. 34. Bus A-phase single-line-to-ground fault.

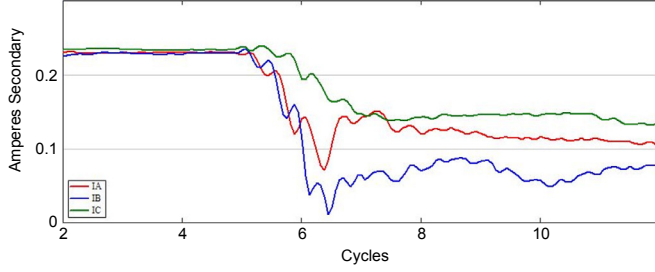


Fig. 35. Bus A-phase-to-B-phase double-line-to-ground fault.

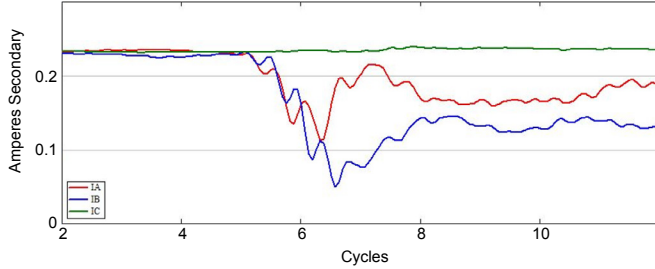


Fig. 36. Bus A-phase-to-B-phase line-to-line fault.

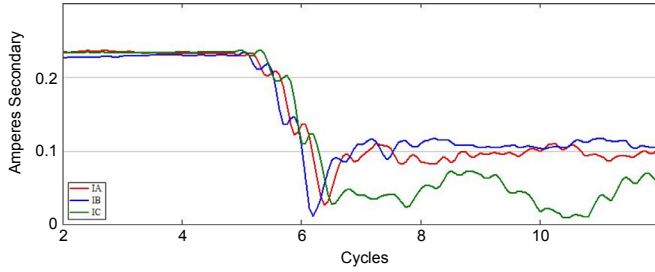


Fig. 37. Bus three-line-to-ground fault.

The differential currents for the bus faults all decreased from the normal steady-state current flow, thereby never exceeding the new pickup.

### B. Adjacent Line Fault

Faults were then applied on the line side of the capacitor on the adjacent line. Fig. 38 to Fig. 41 show the differential current magnitudes.

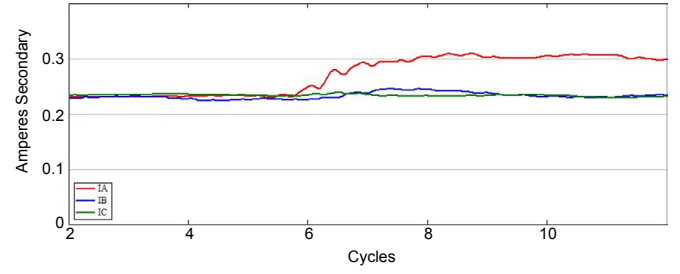


Fig. 38. Adjacent line A-phase single-line-to-ground fault.

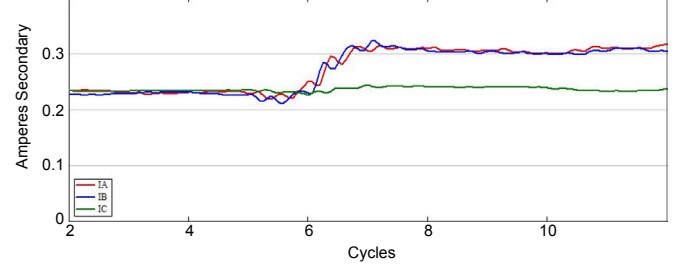


Fig. 39. Adjacent line A-phase-to-B-phase double-line-to-ground fault.

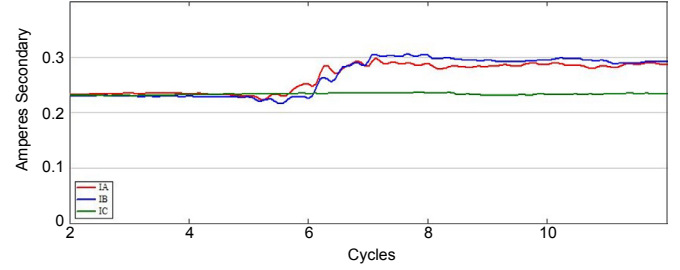


Fig. 40. Adjacent line A-phase-to-B-phase line-to-line fault.

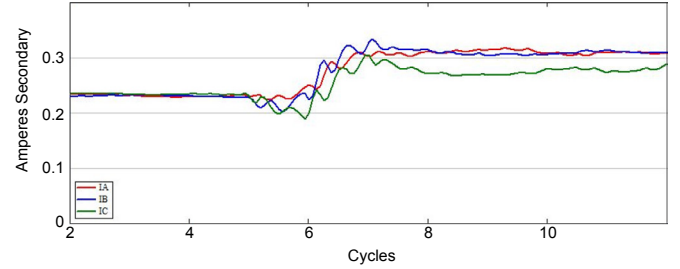


Fig. 41. Adjacent line three-line-to-ground fault.

The differential current increased slightly for all the faults; however, this increase did not come close to the pickup.

## VII. ALPHA PLANE SECURITY

The alpha plane was examined for its behavior during the faults. Due to the light loading and high amount of charging current for these cases (the line is over 100 miles long and capacitive charging current compensation was not available), the alpha plane ratio is just outside the inner radius, as demonstrated in Fig. 42 to Fig. 49. Increasing the line load would further push the ratio into the restraint region.

### A. Bus Fault

Faults were applied on the bus of the substation that contained the series capacitors. In all cases, the ratio oscillated into the restraint region, as shown in Fig. 42 to Fig. 45.



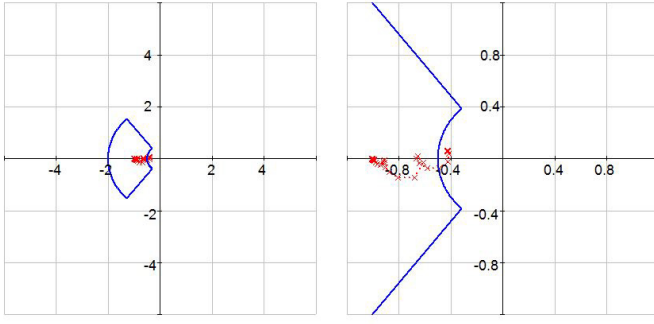


Fig. 42. A-phase single-line-to-ground bus fault.

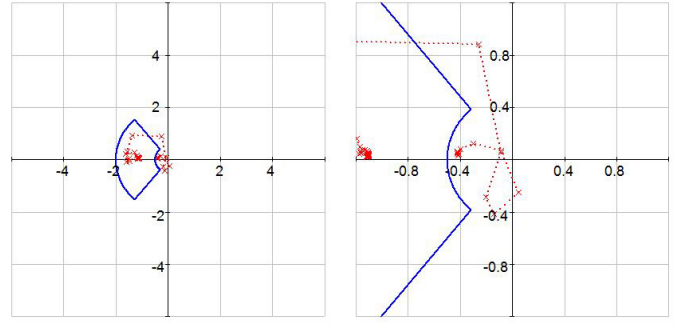


Fig. 46. Adjacent line A-phase single-line-to-ground fault.

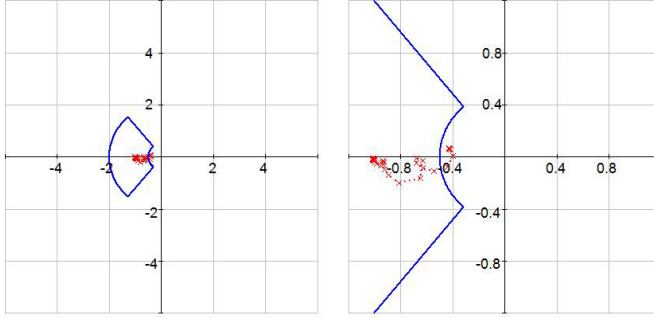


Fig. 43. A-phase-to-B-phase double-line-to-ground bus fault.

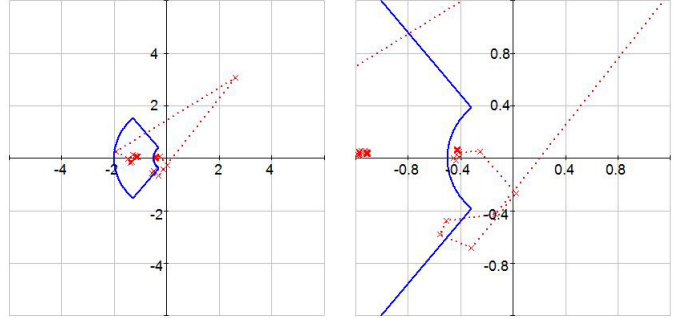


Fig. 47. Adjacent line A-phase-to-B-phase double-line-to-ground fault.

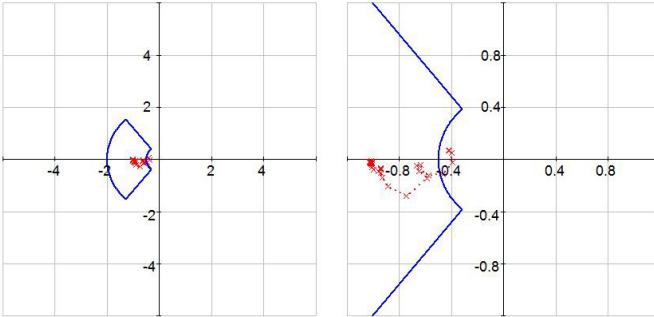


Fig. 44. A-phase-to-B-phase line-to-line bus fault.

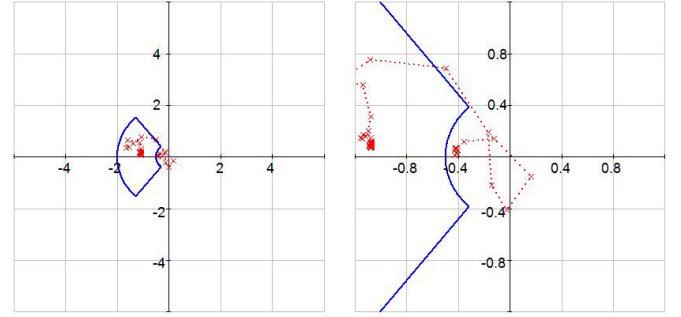


Fig. 48. Adjacent line A-phase-to-B-phase line-to-line fault.

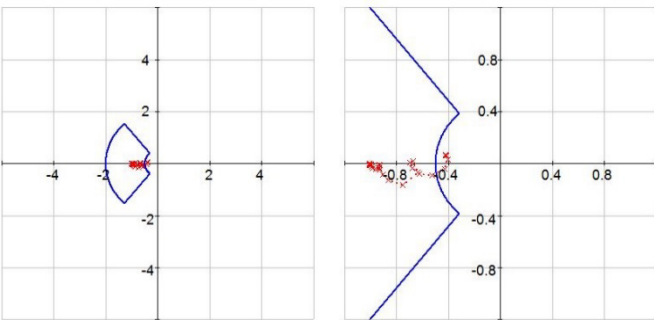


Fig. 45. Three-line-to-ground bus fault.

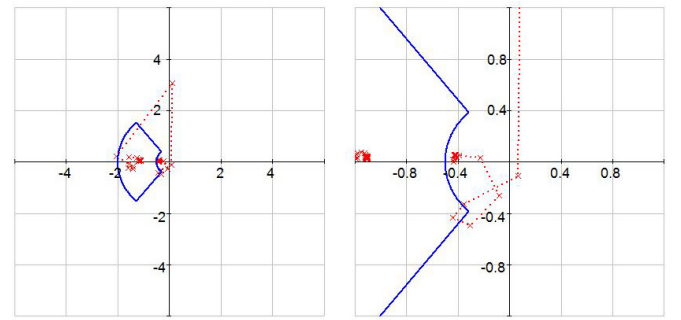


Fig. 49. Adjacent line three-line-to-ground fault.

### B. Adjacent Line Fault

Faults were then applied on the line side of the capacitor on the adjacent line. The alpha plane experienced more oscillations in the operate region before finally settling in the restraint region. Fig. 46 to Fig. 49 show the alpha planes for each fault type.

In all cases, the alpha plane ratio started just outside the inner radius and moved into the restraint region during the fault. This, coupled with the low differential current, makes the differential secure during the external fault conditions.

During testing, two assumptions were made: 1) CT saturation was not possible for adjacent line faults based on analysis performed by Idaho Power, and 2) the communications channels were symmetrical. For a more detailed analysis, refer to [7].



## VIII. BACKUP PROTECTION CONSIDERATIONS

For backup protection, in the event the line current differential scheme is inactive, open breaker transfer trip logic was also added to the line relaying scheme. The line distance relays at the remote noncompensated line terminal will still detect the fault in the forward direction and trip on time delay for the current inversion scenario faults. At the series capacitor line terminal, reverse distance elements with a long time delay that coordinates with other area protection systems and emergency loads were also set that will operate for internal current inversion faults.

## IX. CONCLUSION

This paper has presented the protection challenges and problems on a series-compensated transmission system.

Voltage inversion is mitigated in modern microprocessor-based relays using memory voltage to polarize the distance elements. Voltage inversion also does not negatively impact the negative-sequence and zero-sequence directional elements.

Current inversion affects both the voltage and current profile along the line, rendering distance and directional elements unusable while also decreasing the dependability of differential elements.

For the current differential scheme to be dependable for the internal faults, the phase differential pickup, blocking angle, and restraint radius were decreased. For the scheme to be secure, there must be symmetrical communications channels and no CT saturation.

As power system demand increases, transmission service providers work hard to identify new ways to better use or increase the transfer capability of the existing transmission network. Installing series capacitors is one method for increasing transmission path transfer capability. Increased line compensation levels can result in protection challenges such as voltage or current inversion. This paper demonstrates that joint collaboration among utility engineers, series capacitor bank manufacturers, and relay manufacturers, along with the use of transient simulation and RTDS transient testing, can resolve the challenges of protecting series-compensated lines during voltage or current inversion events.

## X. REFERENCES

- [1] S. Wilkinson, "Series Compensated Line Protection Issues." Available: <http://store.gedigitalenergy.com/FAQ/Documents/Alps/GER-3972.pdf>.
- [2] B. Kasztenny, "Distance Protection of Series Compensated Lines – Problems and Solutions," proceedings of the 28th Annual Western Protective Relay Conference, Spokane, WA, October 2001.
- [3] P. M. Anderson, B. L. Agrawal, J. E. Ness, "Subsynchronous Resonance in Power Systems," IEEE Press, 1990.
- [4] D. L. Goldsworthy, "A Linearized Model for MOV-Protected Series Capacitors," *IEEE Transactions on Power Systems*, Vol. PWRS-2, No. 4, November 1987.
- [5] E. O. Schweitzer, III and J. Roberts, "Distance Relay Element Design," proceeding of the 19th Annual Western Protective Relay Conference, Spokane, WA, October 1992.
- [6] V. Henn, R. Krebs, G. Arruda, R. Dutra, and P. Campos, "High Degrees of Series Capacitors in Bulk Power Transmission Systems Need Special Protection Principles," presented at the 2009 IEEE Bucharest Power Tech Conference, Bucharest, Romania, June/July 2009.

- [7] D. A. Tziouvaras, H. Altuve, G. Benmouyal, and J. Roberts, "Line Differential Protection with an Enhanced Characteristic," proceedings of the 3rd Mediterranean Conference on Power Generation, Transmission, Distribution, and Energy Conversion, Athens, Greece, November 2002.

## XI. BIOGRAPHIES

**Eric Bakie** received a BSEE, with mathematics minor, from the University of Idaho in 2003, a Certificate of Completion in Power System Protection and Relaying from the University of Idaho in 2004, and an MSEE from the University of Idaho in 2010. He joined POWER Engineers as a system studies engineer in 2005. In 2006, he joined Black & Veatch as a substation design engineer. In 2007, he joined Idaho Power Company where he worked as a power production engineer for three years. He is currently working as a system planning engineer with the Idaho Power Company customer operations engineering and construction department. He is a registered professional engineer in the state of Idaho.

**Curtis Westhoff** received his BSEE from the University of Idaho in 2004. After his undergraduate studies, he worked for POWER Engineers as a system studies engineer. In 2006, he joined the system protection department at Idaho Power Company where he worked as a system protection engineer for nine years. In 2015, he received his MSEE from the University of Idaho. Currently he is a senior engineer with the transmission policy and development department of Idaho Power. He is a registered professional engineer in the state of Idaho.

**Normann Fischer** received a Higher Diploma in Technology, with honors, from Technikon Witwatersrand, Johannesburg, South Africa, in 1988; a BSEE, with honors, from the University of Cape Town in 1993; a MSEE from the University of Idaho in 2005; and a Ph.D. from the University of Idaho in 2014. He joined Eskom as a protection technician in 1984 and was a senior design engineer in the Eskom protection design department for three years. He then joined IST Energy as a senior design engineer in 1996. In 1999, Normann joined Schweitzer Engineering Laboratories, Inc., where he is currently a fellow engineer in the research and development division. He was a registered professional engineer in South Africa and a member of the South African Institute of Electrical Engineers. He is currently a senior member of IEEE and a member of ASEE.

**Jordan Bell** received his BS degree in electrical engineering from Washington State University and joined Schweitzer Engineering Laboratories, Inc. in 2008 as a protection engineer in the engineering services department. He performs event report analysis, relay settings and relay coordination, fault studies, and model power system testing using a Real Time Digital Simulator. He is a registered professional engineer in the state of Washington.